NASA TN D-320

TECHNICAL NOTE

D-320

AN EXPERIMENTAL INVESTIGATION OF BOUNDARY-LAYER CONTROL FOR DRAG REDUCTION OF A SWEPT-WING SECTION AT LOW SPEED AND HIGH REYNOLDS NUMBERS

By Donald E. Gault

Ames Research Center
Moffett Field, Calif.

NATIONAL AERONAUTICS AND SPACE ADMINISTRATION
WASHINGTON
October 1960

NATIONAL AERONAUTICS AND SPACE ADMINISTRATION

TECHNICAL NOTE D-320

AN EXPERIMENTAL INVESTIGATION OF BOUNDARY-LAYER CONTROL FOR DRAG REDUCTION OF A SWEPT-WING SECTION AT LOW SPEED AND HIGH REYNOLDS NUMBERS

By Donald E. Gault

SUMMARY

An investigation of laminar boundary-layer control by suction for purposes of drag reduction at low speed and high Reynolds numbers has been conducted in the Ames 12-Foot Pressure Wind Tunnel. The model was a 72.96-inch-chord wing panel, swept back 30°, which was installed between end plates to approximate a wing of infinite span. The airfoil section employed was a modified NACA 66-012 in the streamwise direction. Tests were limited to controlling the flow over only the upper surface of the model. Seventeen individually controllable suction chambers were provided below the surface to induce flow through 93 spanwise slots in the surface between the 0.0052- and 0.97-chord stations.

Tests were made at angles of attack of 0°, ±1.0°, ±1.5°, and -2.0° for Reynolds numbers from approximately 1.5×10^6 to 4.0×10^6 per foot. In general, essentially full-chord laminar flow was obtained for all conditions with small suction quantities. Minimum profile-drag coefficients of about 0.0005 to 0.0006 were obtained for the slotted surface at maximum values of the Reynolds number; these values include the power required to induce suction as an equivalent drag.

INTRODUCTION

Although references 1 and 2 have shown that spanwise flow on a swept wing may adversely affect the stability of the laminar boundary layer and cause premature transition to turbulent flow (relative to flow on an unswept wing), reference 3 indicates that suction boundary-layer control near the leading edge can delay this instability so that transition will occur close to the position of incipient laminar separation (i.e., downstream of minimum pressure). If one is interested in the considerable drag reduction which could result from full-chord laminar flow, a question remains as to the feasibility of maintaining the laminar flow through the region of pressure increase to the trailing edge, particularly for large values of the Reynolds number. Accordingly, an experimental investigation was undertaken in the Ames 12-Foot Pressure

Wind Tunnel to ascertain whether or not full-chord laminar flow and low profile drag could be achieved on a swept wing by means of suction control for a range of Reynolds numbers from approximately 11 to 29 million.

The model employed for the investigation was constructed by aircraft fabrication techniques and had multiple saw-cut slots in one surface. The Norair Division of the Northrop Corporation developed the suction configuration, and designed and constructed the model and related testing equipment.

NOTATION

b_i	average span of suction chamber, measured normal to free-stream direction
c	wing chord in free-stream direction
p_∞	free-stream static pressure
p_i	suction chamber static pressure
p_l	local static pressure on model surface
p_r	total pressure measured by survey-rake tubes
p_t	free-stream total pressure
q_i	volume flow into single suction chamber, based on free-stream conditions
R	Reynolds number, $\frac{U_\infty c}{\nu_\infty}$
S_i	effective reference area, $c \times b_i$
u_m	velocity in boundary layer at 0.997c station (see section entitled "Tests and Procedures")
U	velocity of potential flow at 0.997c station
U_∞	free-stream velocity
x	distance from leading edge measured in free-stream direction
y	distance above airfoil surface measured normal to surface
α	geometric angle of attack
ρ_∞	free-stream mass density

ν_∞ free-stream kinematic viscosity

θ boundary-layer momentum loss thickness at 0.997c station, $\int_0^\infty \frac{u_m}{U}\left(1 - \frac{u_m}{U}\right) dy$ (see section entitled "Tests and Procedures")

C_p pressure coefficient, $\frac{p_l - p_\infty}{(1/2)\rho_\infty U_\infty^2}$

C_{q_i} local suction-flow coefficient of single suction chamber, $\frac{q_i}{U_\infty S_i}$

C_{Q_t} total suction-flow coefficient, $\sum_{i=1}^{i=17} C_{q_i}$

$C_{d_{s_i}}$ coefficient of equivalent drag[1] for the flow in a single suction chamber due to the power required to induce the flow, $C_{q_i}\left[\frac{p_t - p_i}{(1/2)\rho_\infty U_\infty^2}\right]$

C_{d_s} total suction drag coefficient, $\sum_{i=1}^{i=17} C_{d_{s_i}}$

C_{d_w} wake drag coefficient, $2\frac{\theta}{c}\left(\frac{U}{U_\infty}\right)^{3.2}$ (see section entitled "Tests and Procedures")

C_{d_t} total profile drag coefficient (for one surface of the airfoil), $C_{d_s} + C_{d_w}$

Subscript

i the suction chamber number as listed in table II

[1]Assumes: (1) suction air is discharged to the free stream with a velocity U_∞; and (2) efficiencies of suction and discharge systems are equal.

MODEL AND APPARATUS

The model employed for this investigation, was a wing panel, swept back 30°, having both a span and streamwise chord of approximately 7 feet. The airfoil section was a modified NACA 66-012 in the streamwise direction (a thickness ratio of 13.78 percent based on the chord perpendicular to the leading edge). The modifications consisted of a small decrease in leading-edge radius, a short extension forward of the leading edge, and an increase in the trailing-edge angle. Coordinates of the airfoil are listed in table I.

The model was mounted vertically in the Ames 12-Foot Pressure Wind Tunnel between a dummy floor and ceiling as shown in figure 1. In order to approximate conditions representing an infinite span as closely as possible, the dummy floor and ceiling fairings were contoured to the undisturbed streamlines calculated for the infinitely long yawed wing for an angle of attack of 0° (see fig. 2). The model support between these dummy fairings and the tunnel shell were covered with airfoil-shaped fairings to minimize possible disturbing effects.

The model was constructed of aluminum and the waviness of the test surface was less than 0.0003 inch per inch. Surface roughness was minimized by finishing the surface with No. 600 grade emery paper and polishing the resultant surface to a mirrorlike finish with a silicon-base wax.

Boundary-layer control, effected by the pressure difference between the wind tunnel and the atmosphere, was applied to only one surface of the model. Suction was induced through 93 sharp-edged slots normal to the local surface between the 0.0052- and 0.97-chord stations (see table II and fig. 3). The slots were cut through the 0.030-inch outer skin which was bonded to a 0.25-inch continuous inner skin. The induced air passed through the slots into small plenum chambers machined in the inner skin and then through holes drilled from the plenum chamber through the inner skin into 17 large suction chambers. As indicated in table II, one to ten slots were connected to each suction chamber. To ascertain the volume flow nozzles and pressure taps were provided in each suction chamber; these nozzles were calibrated against a standard ASME sharp-edged orifice flowmeter. The induced air passed through the nozzles and a ducting system into a common suction box which contained 17 remotely controlled valves for individual regulation of the flow into each suction chamber. A single master valve between the suction box and the atmosphere, also remotely controlled, provided regulation for the total flow independent of the chordwise suction distribution.

It will be noted in figure 2 that regions of auxiliary suction were provided on both sides of the test surface for which data were obtained. These regions were provided to maintain uniform flow conditions over the test surface. Although the volume flows for the auxiliary regions were

controlled by the 17 valves in the suction box, separate suction chambers and ducts were employed to isolate the flows in the auxiliary region from those measured for the test region.

The model was provided with 24 static-pressure orifices along the midspan of the wing panel for ascertaining the pressure distribution along the test surface. A small microphone was also connected into most of these orifice lines as a means for determining the type of boundary-layer flow passing over the orifice. An additional chordwise row of 8 orifices on each side of the test region was furnished as a means of checking for spanwise pressure gradients.

In order to determine the momentum loss in the boundary layer at the trailing edge for an evaluation of the contribution of the wake drag to the total profile drag, a rake of 6 total-pressure tubes was installed with the leading edge of the tubes at the 0.997-chord station. The rake was constructed of 0.0625-inch outside diameter stainless-steel tubing with the ends flattened to a nominal open height of 0.004 inch. Figure 4 is a photograph of the rake.

A 4 1 3

TESTS AND PROCEDURE

All data were obtained for a nominal tunnel pressure p_t equal to 75 pounds per square inch absolute. Measurements were made for geometric angles of attack of 0°, $\pm 1.0^\circ$, $\pm 1.5^\circ$, and -2.0° for a range of dynamic pressures which varied from approximately 15 to 100 pounds per square foot. Under these conditions the Reynolds number per foot varied from about 1.5×10^6 to 4×10^6; the Mach number never exceeded 0.12.

In general, the following test procedure was employed throughout the investigation: With a given angle of attack and an arbitrary value of dynamic pressure (Reynolds number), gross variations were made in the chordwise suction distribution until essentially full-chord laminar flow was established as determined by listening to the output from the microphones connected to the static orifices. The sounds emanating from the laminar, transitional, and turbulent flow were distinctive and permitted a rapid determination of the type of boundary-layer flow occurring along the airfoil surface. Once approximately full-chord laminar flow was established, the volume flow into each suction chamber was reduced to an absolute minimum value consistent with the maintenance of 100-percent laminar flow. All data and measurements for this minimum suction distribution were then photographically recorded from a multiple-tube manometer board. Additional records were also obtained with similar chordwise distributions of suction for increased and decreased levels of total suction quantity (relative to the initial minimum setting).

An important pretest procedure was the careful inspection and maintenance of the test surface and slots. Removal of all dust particles and foreign material from the slots and surface was imperative for achieving full-chord laminar flow.

It should be emphasized that the wake drag coefficient was calculated using Squire's relationship for an unswept wing (ref. 4).

$$C_{d_w} = 2\frac{\theta}{c}\left(\frac{U}{U_\infty}\right)^{3.2}$$

where the boundary-layer momentum-loss thickness θ was evaluated from the wake survey data by means of the expression

$$\frac{u_m}{U} = \sqrt{\frac{p_r - p_l}{p_t - p_l}}$$

A 4 1 3

to determine the velocity profiles. This procedure effectively assumes that the boundary-layer crossflow was negligible in comparison to the flow in the free-stream direction. Notwithstanding the considerable inhibiting effect of suction control on the spanwise boundary-layer flow, complete elimination of the crossflow components was not possible. As a result, there are two sources for error in the values of the wake drag coefficient, one resulting from the neglect of the crossflow component of momentum loss and a second arising from the inability of the survey rake to provide an indication of the two local total pressures p_r if the axes of the tubes were misalined more than, say, 10° with the direction of the local resultant velocity. An analysis of these errors, however, has indicated that Squire's relationship as applied herein provides a good but conservative estimate (larger values) for the values of the wake drag coefficient. It is to be noted that the wake drag never exceeded about 30 percent of the total profile drag; any errors in the wake drag, therefore, would represent only a small error in the total profile drag.

RESULTS AND DISCUSSION

Chordwise Pressure Distribution

Typical chordwise distributions of pressure at the midspan of the model are shown in figure 5 for the various angles of attack. As long as essentially 100-percent laminar flow was maintained, changes in Reynolds number and suction had a negligible influence on these distributions.

Chordwise Suction-Flow Distributions

Illustrated in figure 6 are three representative chordwise suction distributions; the conditions shown are, approximately, those required for obtaining the minimum value of the total profile drag coefficient for the specified angles of attack and Reynolds numbers. It is apparent, as should be expected, that the suction requirements were highest over the rear of the airfoil - the region of strong adverse pressure gradients and crossflow in the boundary layer. A relatively low and constant level of suction was required along the forward portion of the airfoil but it is to be noted that the maintenance of laminar flow became increasingly sensitive to suction quantity near the leading edge as the angle of attack increased in either the positive or negative direction. The change in the angle of attack from 0° to $\pm 1.5^\circ$, shown in figure 6, increased the required suction flow near the leading edge. For the positive angle, the increase is probably the result of the destabilizing influence of the localized pressure peak at the leading edge (fig. 5). The increase in suction for the negative angle probably reflects the generally destabilizing effects of the increase in boundary-layer cross flow with the increase in the pressure coefficients on the swept wing.

Drag

Some variations of the total profile drag coefficient C_{d_t} with flow coefficient are presented in figure 7. The two-component coefficients C_{d_w} and C_{d_s} (wake and suction drag, respectively) are also shown. For a given angle of attack, Reynolds number, and suction distribution, the suction drag coefficient, of course, increased continuously with increased suction flow coefficient, the variation being approximately linear. The wake drag component, in contrast, usually decreased continuously with increased flow although in some instances it attained a minimum value and subsequently increased. In these latter instances, excessive suction apparently was destabilizing to the laminar boundary layer and prevented achieving full-chord laminar flow. The resultant total profile drag coefficients attained a definite minimum value at some optimum rate of suction flow; insufficient suction precluded the possibility of achieving full-chord laminar flow, and excessive suction was extravagant from suction power requirements and sometimes caused transition to turbulent flow at some forward station on the airfoil.

A summary of the drag data for this investigation is shown in figure 8 wherein the minimum values obtained for total profile drag coefficients are presented for all angles of attack as functions of the Reynolds number. In all cases the minimum drag coefficients decrease at first with increasing Reynolds number, the trend paralleling the decrease predicted by theory for the laminar boundary layer on a flat plate. Since an increase in Reynolds number thins the boundary layer and reduces the

required suction flow, one might expect such a decrease in the total profile-drag coefficient. In all cases, however, above a certain value of Reynolds number the drag coefficients began to increase; the increase was particularly abrupt for -2.0°. These increases in the minimum total profile drag coefficients occurred when the stream Mach number reached a value of about 0.1. It is known that, although the turbulent velocity fluctuations due to vorticity in the wind-tunnel air stream are extremely low,[2] the noise level in the wind tunnel increases rapidly with increasing velocity and attains and exceeds values of 125 decibels for Mach numbers greater than about 0.1. The destabilizing influence of such noise levels coupled with the high values of the Reynolds number per foot of this investigation (up to 4×10^6) are believed to be the probable cause of the drag increases shown in figure 8.

It should be emphasized that for most of the drag data shown in figure 8, no turbulent or transitional-type boundary-layer flow could be detected at the most rearward microphone station of 0.97 chord. It is possible that transition began in the remaining short distance to the trailing edge and, since transitional flow was actually detected at the 0.97 chord station in a few instances, the drag data of figure 8 correspond to conditions of what should be termed essentially full-chord laminar flow.

Ames Research Center
National Aeronautics and Space Administration
Moffett Field, Calif., Mar. 8, 1960

REFERENCES

1. Gray, W. E.: The Effect of Wing Sweep on Laminar Flow. R.A.E. Tech. Memo. Aero 255, 1952.

2. Owen, P. R., and Randall, D. G.: Boundary Layer Transition on a Sweptback Wing. R.A.E. Tech. Memo. Aero 277, 1952.

3. Anscombe, A., and Butler, S. F. J.: The Effect of Sweepback on the Laminar Boundary Layer. Interim Note on Current Experiments With Leading Edge Suction. R.A.E. Tech. Memo. Aero 351, 1953.

4. Schlicting, Hermann: Boundary Layer Theory. McGraw-Hill Series in Mechanical Engineering, 1955, pp. 512-513.

[2]The fluctuations (for wind-tunnel conditions of the present investigation) are so low that they have not been resolved with the available hot-wire anemometer equipment. It is known, however, that the root mean square of the longitudinal component of the velocity fluctuations can be no greater than something of the order of 0.01 percent of the free-stream velocity.

TABLE I.- AIRFOIL COORDINATES BASED ON A SECTION PERPENDICULAR TO THE LEADING EDGE

Chordwise station, percent chord	Airfoil ordinate, percent chord
0	0
.5482	.9745
.8224	1.1636
1.2335	1.3939
2.4671	1.9312
5.2786	2.8506
7.7713	3.4768
10.2641	4.0072
15.2494	4.8607
20.2347	5.5129
25.2200	6.0163
30.2054	6.3962
35.1907	6.6664
40.1760	6.8319
45.1613	6.8917
50.1467	6.8508
55.1320	6.6973
60.1173	6.3992
65.1026	5.8588
70.0881	5.1269
75.0734	4.2694
80.0587	3.3661
85.0440	2.4605
90.0294	1.5404
95.0147	.6880
100.	0
Leading-edge radius: 0.81 percent chord	

TABLE II.- DIMENSIONS AND DETAILS OF SLOTS AND SUCTION CHAMBERS

Slot no.	Slot position, x/c	Slot width, in.	Plenum chamber holes[1], dia. in.	Suction chamber no.	Slot no.	Slot position, x/c	Slot width, in.	Plenum chamber holes[1], dia. in.	Suction chamber no.
1	0.0052	0.004	0.1000	1	48	0.7232	0.005	0.0315	12
2	.0207	↓	.1000	2	49	.7287	↓	.0380	13
3	.0497		.1000	3	50	.7342		.0365	↓
4	.0892		.0350	4	51	.7397		.0355	
5	.1296		.0350	5	52	.7452		.0345	
6	.1698		.0330	6	53	.7506		.0340	
7	.2050		.0350	6	54	.7561		.0335	
8	.2500		.0260	7	55	.7616		.0330	
9	.2985		.0300	7	56	.7671		.0325	
10	.3331		.0260	8	57	.7726		.0325	
11	.3616		.0265	↓	58	.7781		.0385	14
12	.3854		.0270		59	.7836		.0375	↓
13	.4060		.0280		60	.7890		.0365	
14	.4249		.0255	9	61	.7945		.0360	
15	.4431		.0260	↓	62	.8000		.0350	
16	.4599		.0265		63	.8055		.0345	
17	.4757		.0265		64	.8110		.0340	
18	.4904		.0270		65	.8165		.0335	
19	.5041		.0275		66	.8219		.0330	
20	.5175		.0280		67	.8274		.0390	15
21	.5302		.0245	10	68	.8329		.0380	↓
22	.5420		.0245	↓	69	.8384		.0370	
23	.5534		.0245		70	.8439		.0365	
24	.5639		.0245		71	.8494		.0355	
25	.5743		.0250		72	.8548		.0350	
26	.5846		.0250		73	.8603		.0345	
27	.5946		.0255		74	.8658		.0340	
28	.6045		.0260		75	.8713		.0335	
29	.6141		.0260		76	.8768		.0390	16
30	.6233		.0260		77	.8823		.0380	↓
31	.6300	.005	.0360	11	78	.8877		.0375	
32	.6355	↓	.0345	↓	79	.8932		.0365	
33	.6410		.0335		80	.8987		.0360	
34	.6465		.0325		81	.9042		.0350	
35	.6519		.0315		82	.9097		.0345	
36	.6574		.0310		83	.9152		.0340	
37	.6629		.0305		84	.9207		.0335	
38	.6684		.0300		85	.9261		.0390	17
39	.6739		.0300		86	.9316		.0380	↓
40	.6794		.0370	12	87	.9371		.0375	
41	.6848		.0360	↓	88	.9426		.0365	
42	.6903		.0345		89	.9481		.0360	
43	.6958		.0335		90	.9536		.0355	
44	.7013		.0330		91	.9590		.0350	
45	.7068		.0325		92	.9645		.0345	
46	.7123		.0320		93	.9700		.0340	
47	.7177		.0315						

[1]Four holes per inch spanwise

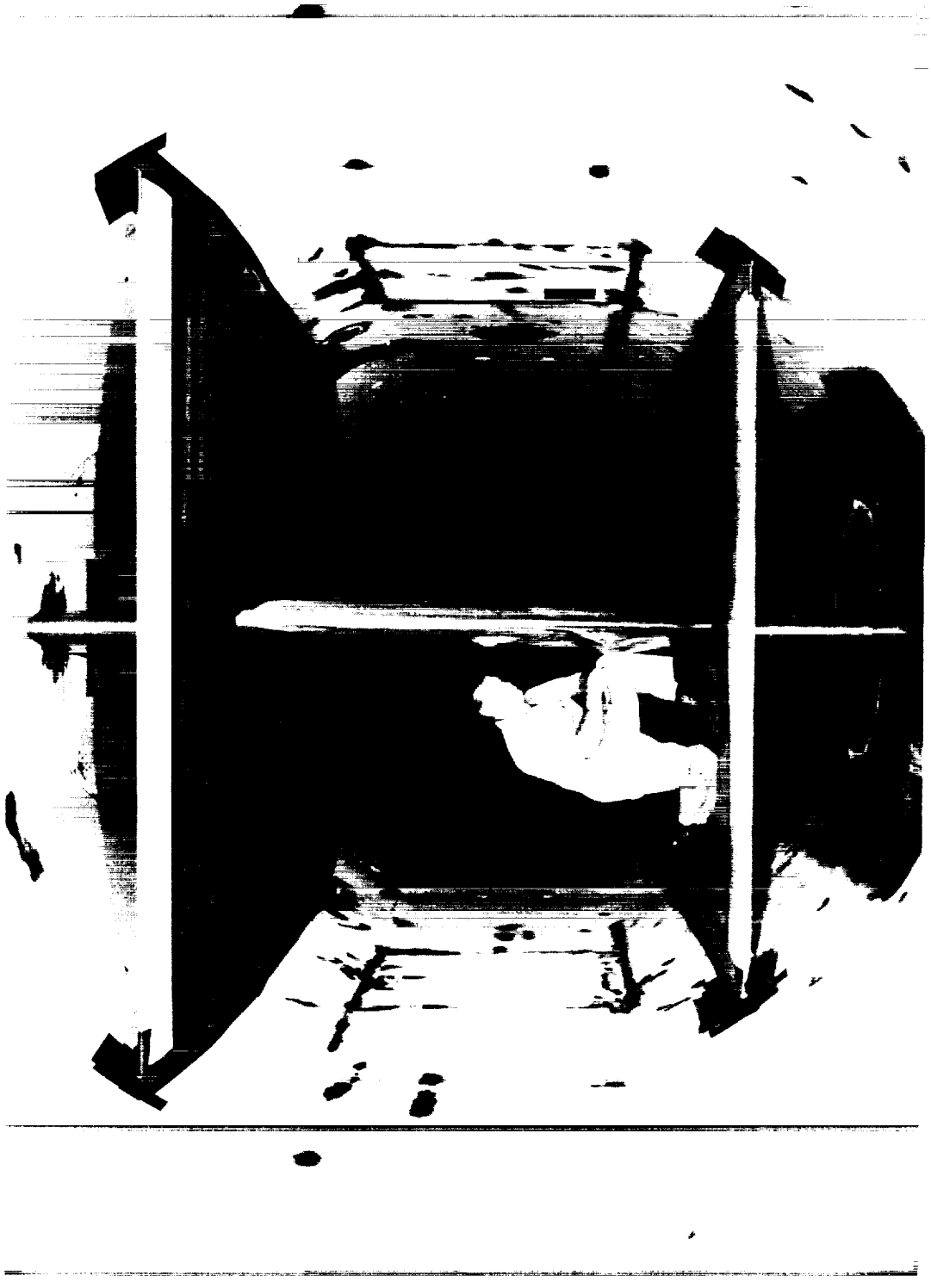

A-25391

Figure 1.- The model installed in the Ames 12-Foot Pressure Wind Tunnel.

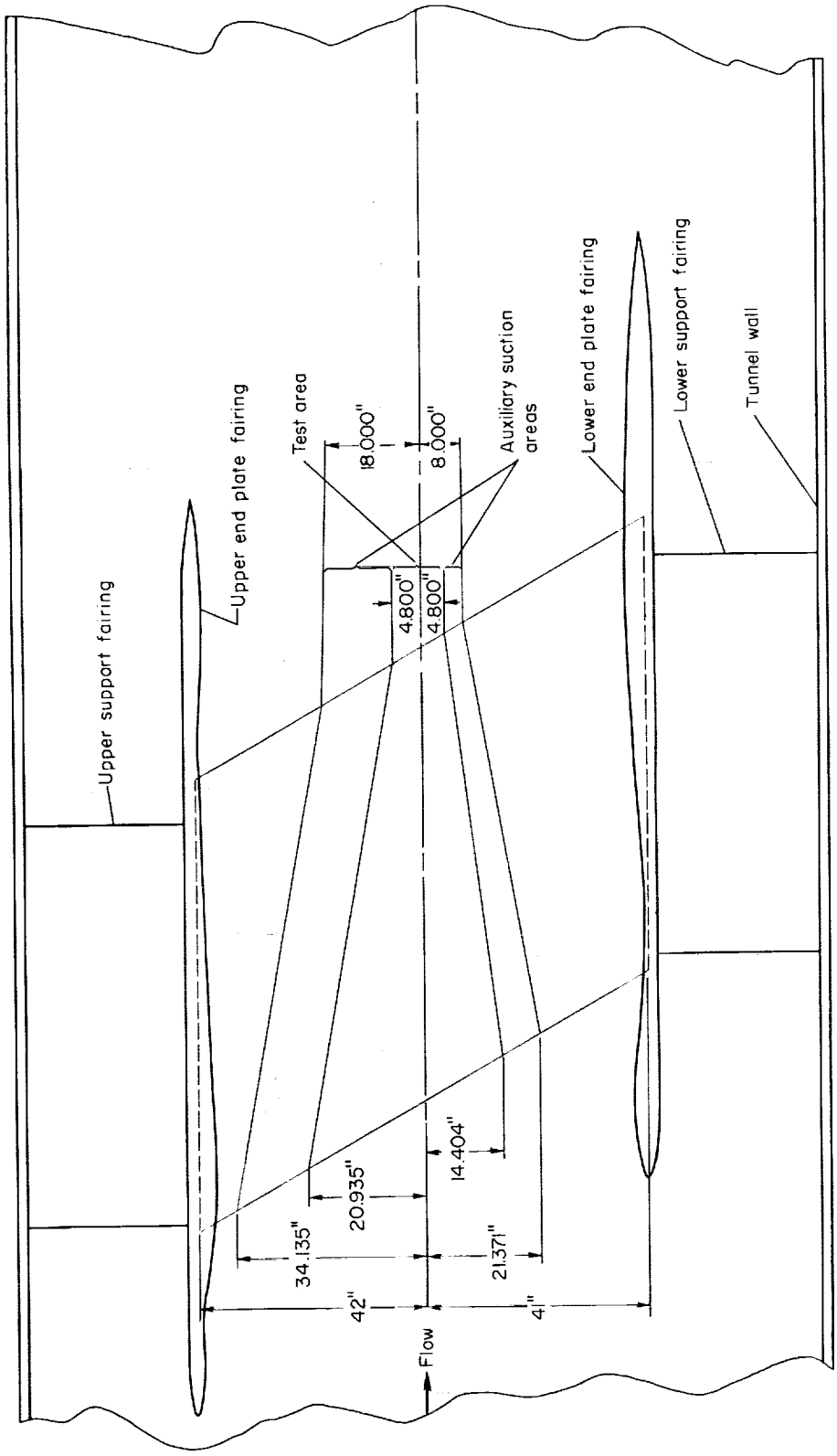

Figure 2.- Dimensional details of the model and wind-tunnel installation.

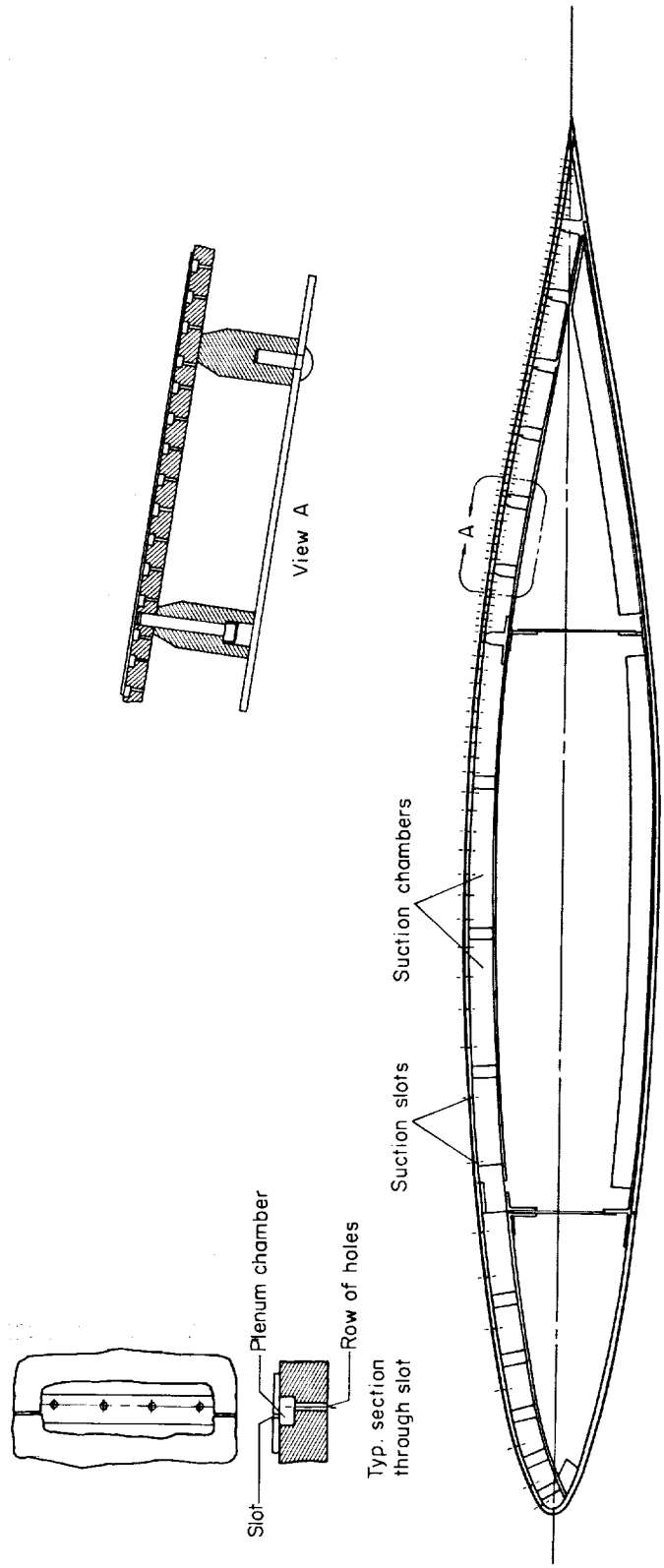

Figure 3.- Details of the suction slots and suction chambers.

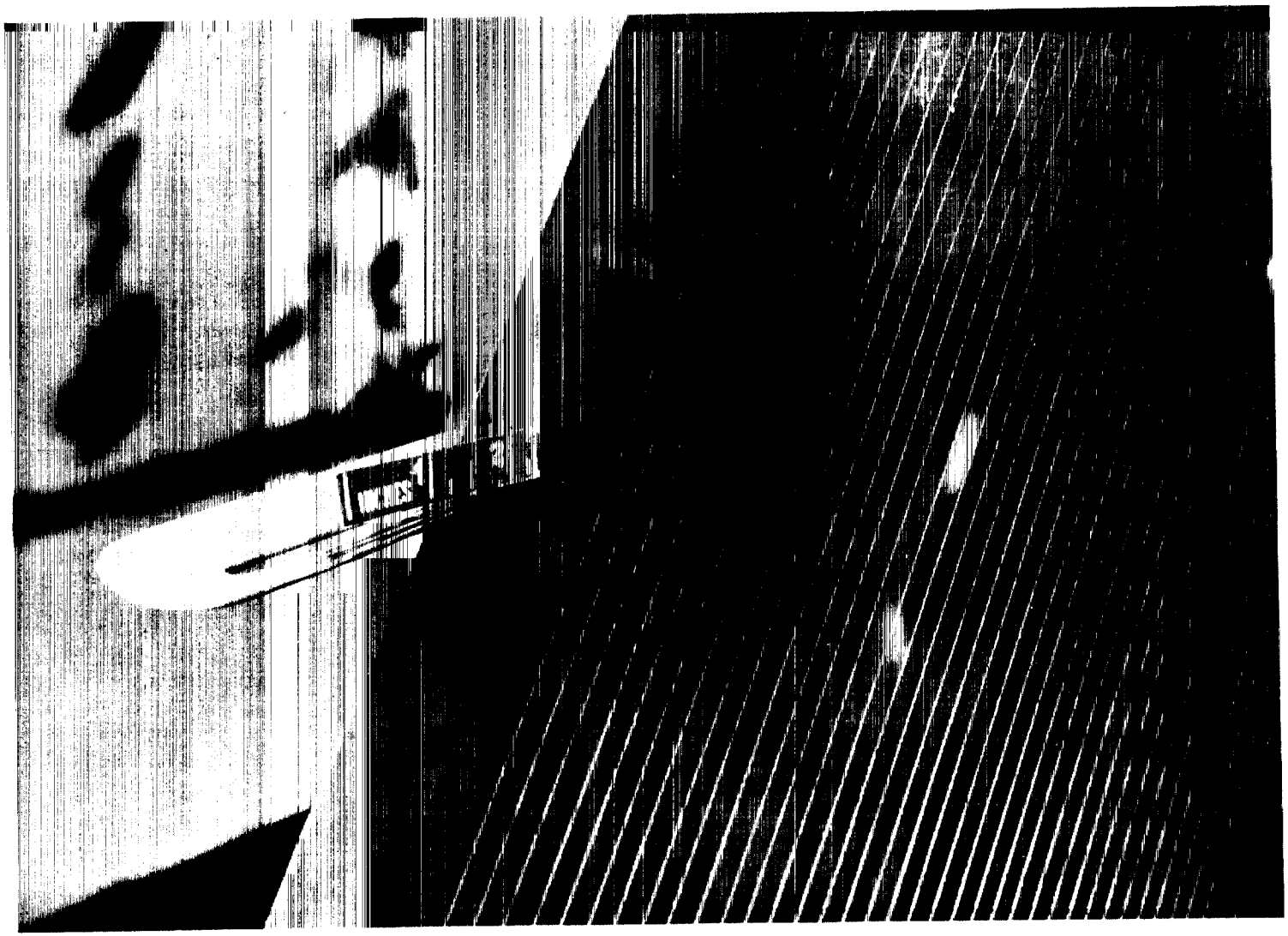

A-25393

Figure 4.- Photograph of the boundary-layer survey rake.

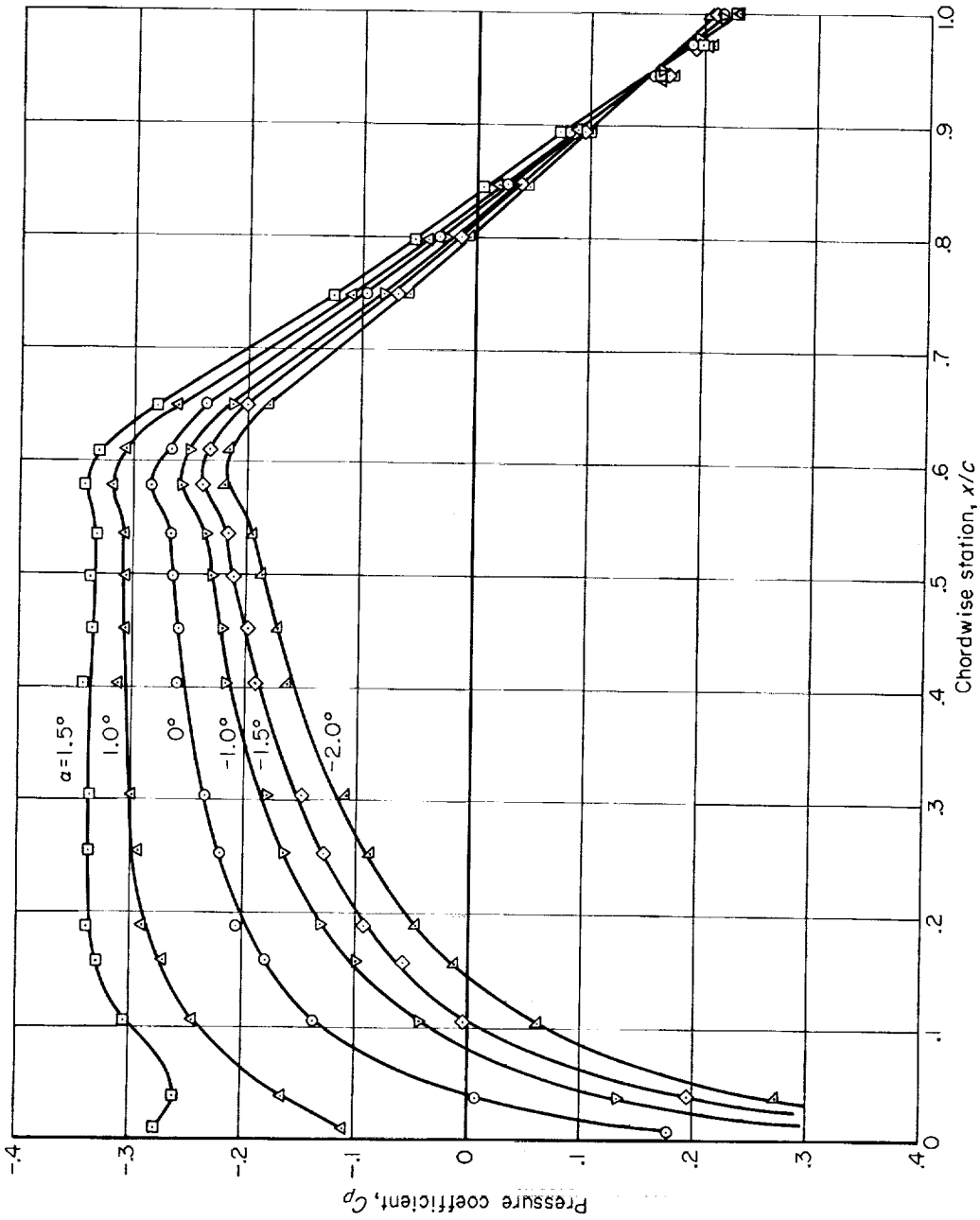

Figure 5.- Typical pressure distributions for the upper surface at the midspan of the model for various angles of attack.

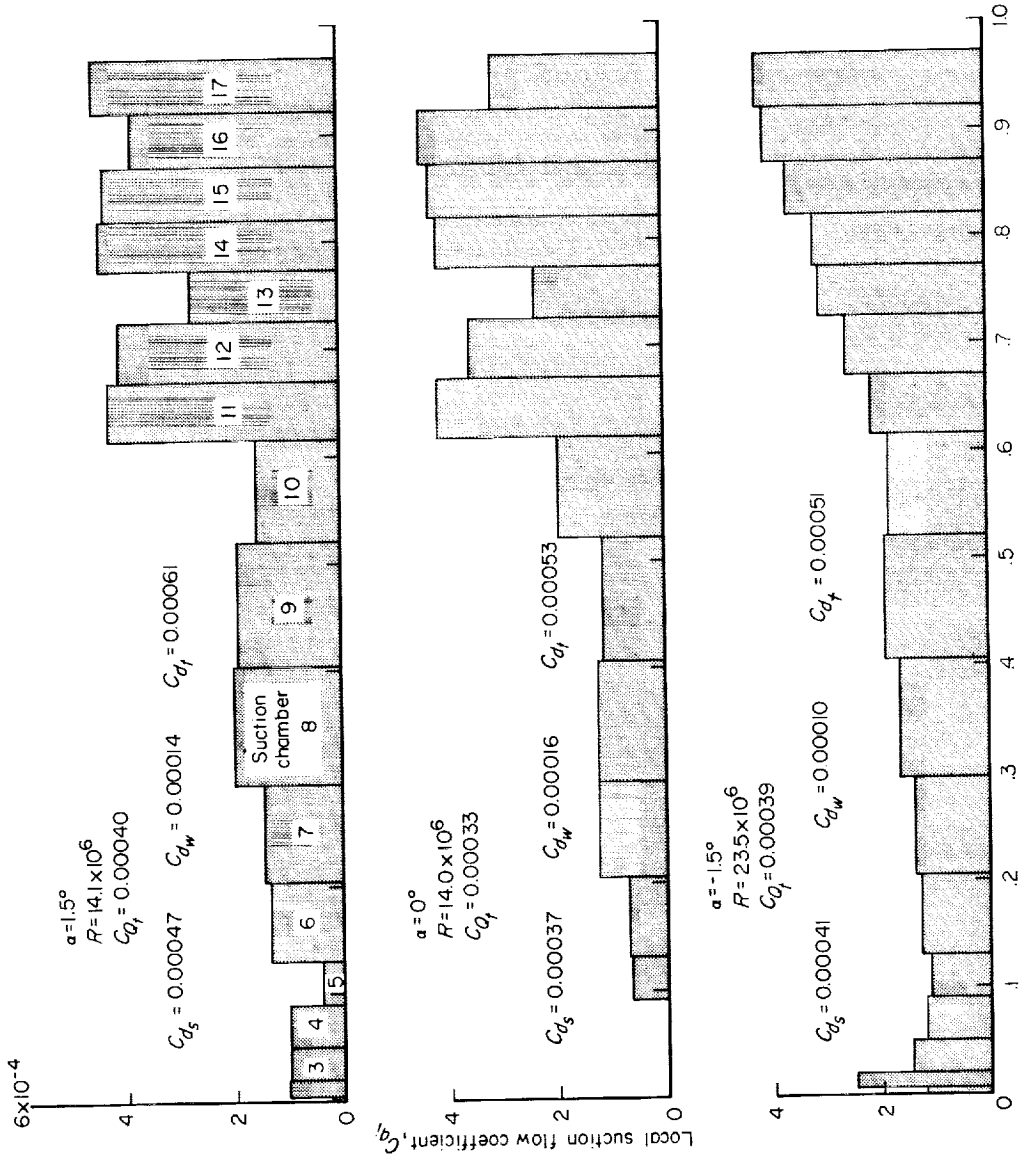

Figure 6.- Typical chordwise distributions of the suction flow for the upper surface.

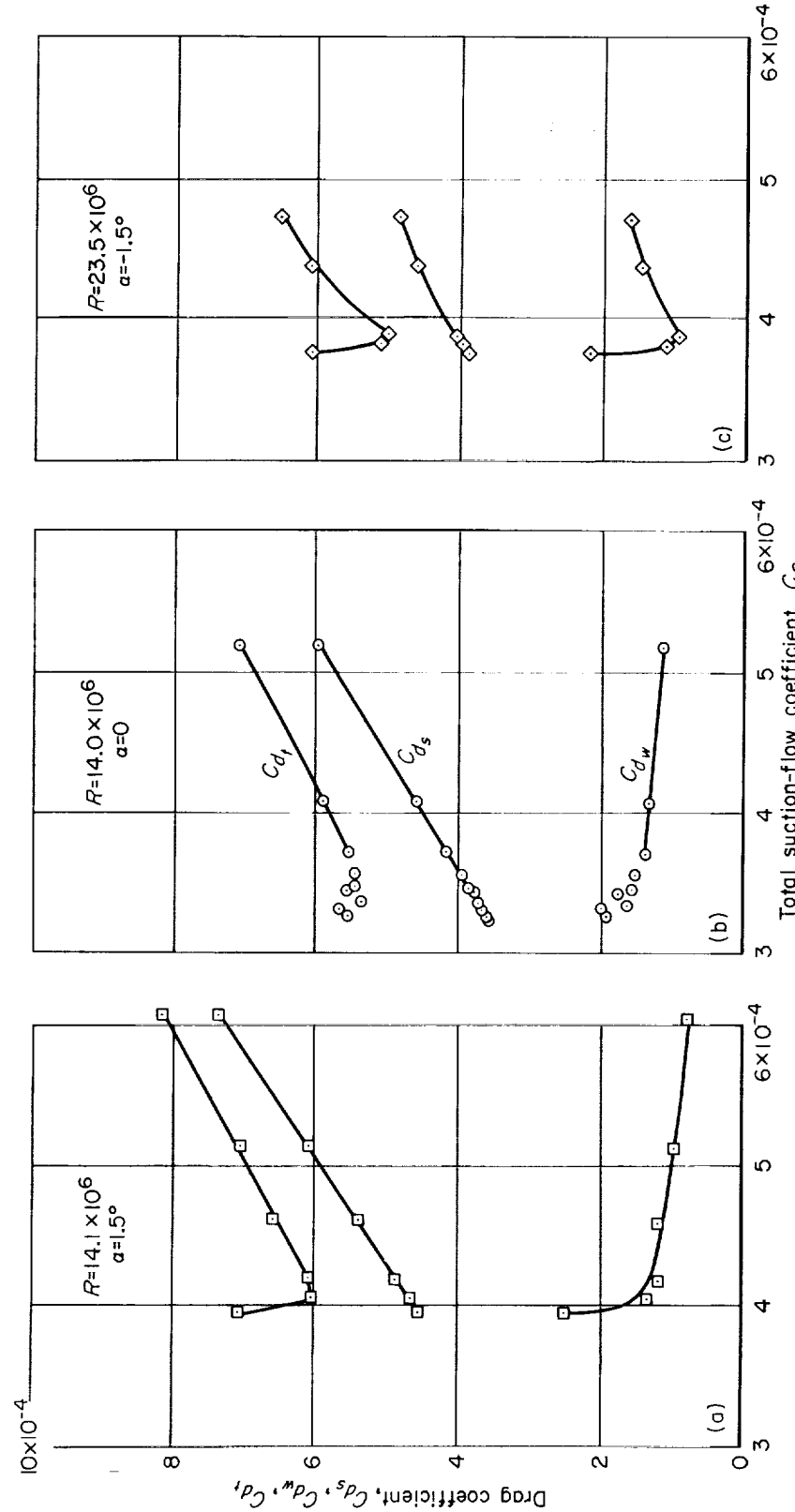

Figure 7.- Typical variations of the drag for the upper surface with suction flow.

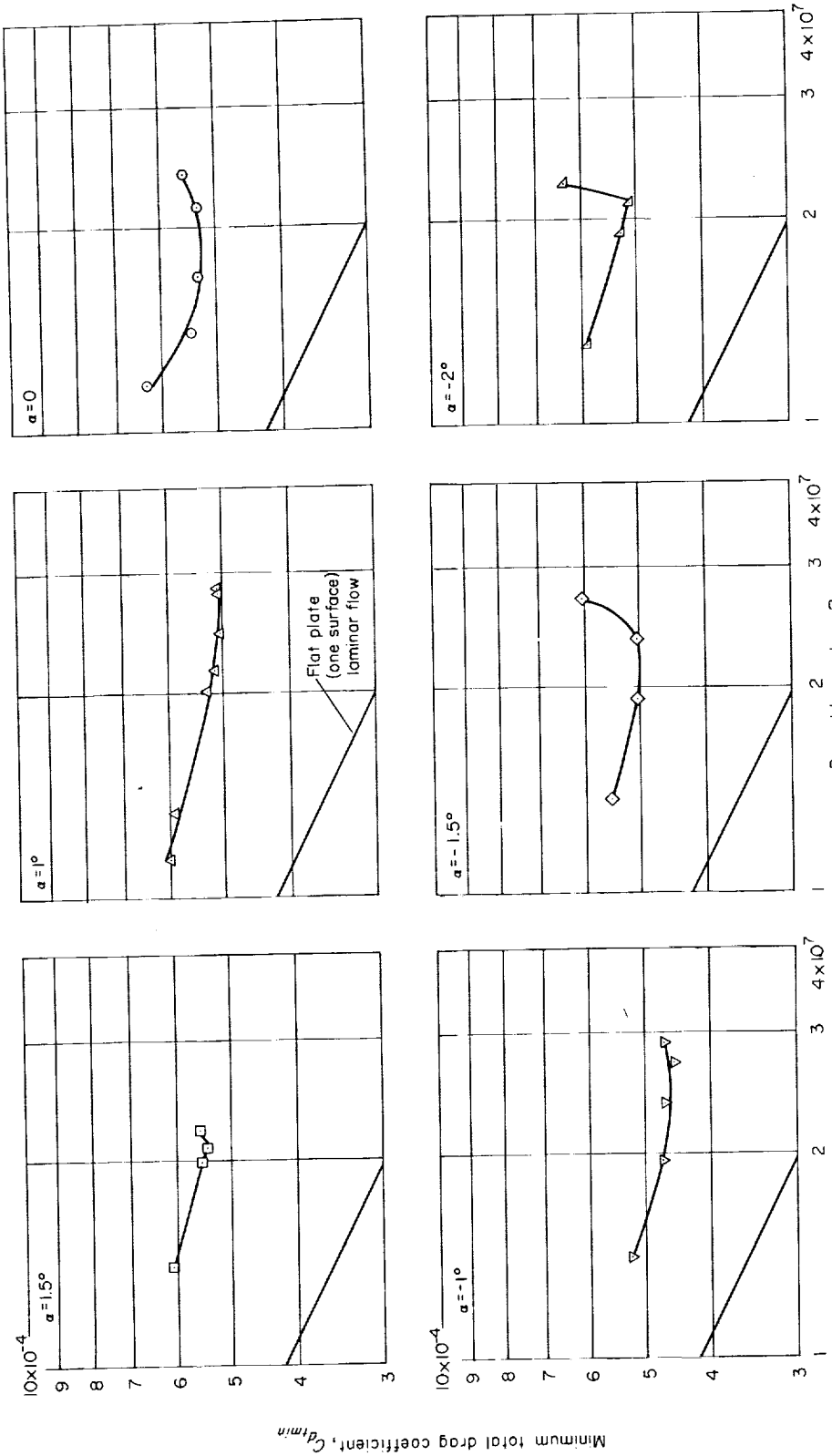

Figure 8.- Variation of the minimum total drag for the upper surface with Reynolds number.